ELESTRES: PERFORMANCE OF NUCLEAR FUEL, CIRCUMFERENTIAL RIDGING, AND MULTIAXIAL ELASTIC-PLASTIC STRESSES IN SHEATHS

M. Tayal

Atomic Energy of Canada Limited,
CANDU Operations
Sheridan Park Research Community
Mississauga, Ontario, Canada, L5K 1B2

ABSTRACT

The finite element code ELESTRES models the two-dimensional axisymmetric behaviour of a CANDU fuel element during normal operation. The main focus of the code is to estimate temperatures, fission gas release, and axial variations of deformations/stresses in the pellet and in the sheath. Thus the code is able to predict details like stresses/strains at circumferential ridges.

This paper describes the current version of ELESTRES. The emphasis is on a recent addition: multiaxial stresses in the sheath near circumferential ridges. For accuracy in the critical region, a fine mesh is used near the ridge. To keep computing costs low, a coarse mesh is used near the midplane of the pellet.

Predictions of ELESTRES show good agreement with about 80 measurements of fission-gas-release. In this paper, we also present ELESTRES predictions of hoop strains in sheaths, for two irradiations: element ABS and bundle GB. For both irradiations, predictions compare favourably with measurements. An illustrative example shows that near circumferential ridges, bending contributes to multiaxial stresses in the sheath. This can have a significant effect on sheath integrity, such as during stress-corrosion-cracking due to power-increases, or during corrosion-assisted-fatigue due to power-cycling.

1. INTRODUCTION

Figure 1 shows the geometry of a CANDU* fuel bundle. Figure 2 shows a fuel element. The two figures also illustrate some terms relevant to this paper. The bundle contains 20-40 cylindrical fuel sheaths made of Zircaloy-4. Each sheath contains 20-40 pellets of UO_2, which produce heat in the reactor. The sheaths provide a barrier against release of radioactive fission products to the surrounding coolant. Hence the integrities of the sheath and of the sheath/endcap weld, are important considerations in the design of fuel elements.

The computer code ELESTRES[1] models the thermal and mechanical behaviour of an individual fuel element, during its irradiation life under normal operating conditions.

---

* CANDU - CANada Deuterium Uranium - is a registered trademark of Atomic Energy of Canada Limited.

The present paper describes the current version of ELESTRES. In this paper, the focus is on calculating multiaxial elastic-plastic stresses in the sheath near the circumferential ridges. We first list the objectives/results/uses of ELESTRES. Then we summarize the evolution of ELESTRES, and related past work. This is followed by an overview of the major physical processes included in ELESTRES, and how they are linked. Then we give the details of three selected features of the code: transient temperatures; multiaxial stresses in the sheath; and creep of Zircaloy. This is followed by some comparisons of predictions vs measurements from irradiations. Finally, two illustrative examples are given.

2. APPLICATIONS OF ELESTRES

The following are the main parameters calculated by ELESTRES:

(i) Temperatures along the radius of the pellet and the sheath.

(ii) Fission gas release and the associated internal gas pressure.

(iii) Circumferential ridging: Circumferential ridging of the sheath is a result of axially-non-uniform, radial expansion of the pellet. Expansion of the pellet is a major source of stresses and strains in sheaths, and in sheath/endcap welds. Stresses should be kept low to avoid failure by stress-corrosion-cracking. Strains should be kept low to avoid rupturing the sheath. High strains can also lead to channelling[2] of dislocations. This can anneal the hardening due to irradiation. If this occurs at a localized spot, e.g. at circumferential ridges, then a weak spot is created in the sheath. Subsequent strains due to, say fission gas, can then concentrate at the weak spot, rendering the sheath more prone to failure.

(iv) Stress-corrosion-cracking: This may occur due to the combined effects of stresses due to power-increase, and of corrodants in the fission-products. ELESTRES includes an estimate for the probability of fuel failure due to stress-corrosion-cracking, based on an empirical correlation.

The development of ELESTRES was initially sponsored by Atomic Energy of Canada Limited, to predict fuel behaviour during normal operation. The objective is to assess if fuel of a given design will survive the intended environment (e.g. power, burnup) during normal operation. This is done by calculating temperatures to check for melting, by calculating internal pressure to check for bursting, and by calculating hourglassing to check for overstrain. Other uses of ELESTRES include: calculating fission gas release for subsequent use in analyses of sheath strain during hypothetical accidents; and calculating pellet expansion for subsequent use in assessments of stresses near welds between sheaths and endcaps. Thus, ELESTRES has been used for the following applications, either by itself or in conjunction with other codes like FEAST[3] and ELOCA[4]:

- Determine the impact on fuel performance of: pellet density; surface roughness; shape and length of the pellet.

- Calculate the power that can cause central melting during abnormal operation.

- Determine the pattern of multiaxial stresses and strains near circumferential ridges.

- Assess the impact of power cycling, on fatigue of the sheath near circumferential ridges.

- Assess the pattern of stresses near sheath/endcap welds, in an effort to identify and remove the cause of fuel failures[5] in the Bruce reactor.

- Determine the acceptable distribution of unbonded areas in endcap welds.

- Predict the performance of fuel during hypothetical transients involving: Loss of Reactivity Control; Loss of Main Feedwater; and Loss of Coolant.

- Predict the probability of fuel failure, during multiple ramps in power.

Reference 6 discusses some of the above applications.

3. EVOLUTION OF ELESTRES

Before we describe the details of ELESTRES, we give a summary of its predecessor, ELESIM[7]. Over the years, ELESIM[7] has been frequently used for modelling the performance of CANDU fuel during normal operation. Its constituent models are physically (rather than empirically) based, and include such phenomena as: heat transfer between the pellet and the sheath; influence of temperature, and of changes in porosity/density, on the thermal conductivity of the pellet; effect of burnup on the radial distribution of neutron-flux; fission gas release as a function of microstructure and of irradiation; densification of UO_2 as a function of time and temperatures; swelling of UO_2 due to fission products; and creep of the sheath as a function of stress, of temperature, and of neutron-dose. ELESIM has been verified[7] extensively against numerous irradiations in experimental and in commercial reactors.

ELESTRES retains all the preceding sub-models of ELESIM. In addition, ELESTRES also calculates the deformation of the pellet, by a two-dimensional, axisymmetric, finite-element model. The calculations include the effects of thermal, elastic, plastic, and creep strains. Cracking is also simulated. The pellet calculations use an earlier version of the FEAST code[3].

ELESTRES continues to provide the information provided by ELESIM, on temperatures and on fission-gas-release. In addition, ELESTRES also provides information on circumferential ridging, and, to a limited extent, on stress-corrosion-cracking.

The first version of ELESTRES was introduced in 1977. Reference 7 gives the details of those portions of ELESTRES that are common with ELESIM. Reference 3 describes the details of the finite element model

FEAST, whose earlier version was used in ELESTRES for calculating pellet deformations. Reference 1 describes how the two major parts, ELESIM and FEAST, were combined in the initial version of ELESTRES. Reference 6 describes some recent applications of ELESTRES, in design/analysis of CANDU fuel.

The current version of ELESTRES contains improvements over the original, in the following major areas: sheath stress; yield strength of the pellet; creep rate of Zircaloy; transient temperatures; calculations at end-of-life; ANS 5.4 correlation for gap inventory; densification of UO_2; and additional conveniences in input/output/interfacing with other codes.

For brevity, this paper focuses on the first improvement listed above: multiaxial elastic-plastic stresses in the sheath. To provide a perspective, however, we first give an overview of the various physical processes included in ELESTRES, and how they are linked.

4. OVERVIEW: PHYSICAL PROCESSES

4.1 Temperatures

In ELESTRES, the neutron flux is allowed to be non-uniform along the radius of the pellet: it is normally higher near the outer surface, and lower near the center. Further, the distribution of neutron flux, along the radius of the pellet, is a function of pellet diameter, of UO_2 enrichment, and of burnup. ELESTRES also accounts for the build-up of plutonium near the outer surface of the pellet.

ELESTRES assumes that the heat transfer coefficient between the sheath and the pellet is a function of: radial gap/contact-pressure between the pellet and the sheath; the composition of gases inside the fuel element; and the initial roughnesses of the surfaces of the sheath and of the pellet. ELESTRES allows the first two parameters above to change continuously during irradiation. For example, the pellet first expands thermally, then shrinks due to densification, then swells due to solid fission products (discused later). The sheath creeps due to coolant pressure. Thus the diametral clearance/contact-pressure, between the pellet and the sheath, changes continuously, not only for the preceding reasons, but also due to changes in power. As more fission gases are released from the pellet, the composition of gas changes inside the fuel element. All these effects combine to give a complex variation of heat transfer coefficient between the pellet and the sheath, during the residence of fuel in the reactor. ELESTRES will predict the resulting distribution of temperatures, normally highest at the center and lowest near the pellet/sheath interface.

4.2 Fission Gas Release

Irradiation generates fission products within the grains of UO_2. Some of the fission products are gaseous. The gas is assumed to diffuse through UO_2 grains; ELESTRES uses Booth's 'equivalent sphere' model[8] for this calculation. The amount of diffusion to grain-boundaries depends, among others, on the local temperature and on the size of the grain. The diffused gas accumulates in grain-boundary bubbles. The bubbles grow as

more gas reaches the grain boundary, either by diffusion or during grain-boundary sweeping due to grain growth (equiaxed and columnar). ELESTRES assumes that a change in power generates thermal stresses in the pellet. This produces microscopic (and macroscopic) cracks in the pellet. The cracks provide a path, called tunnels, between the grain-boundaries and the pellet/sheath gap. When the bubbles grow big enough to touch each other (i.e. to interlink), any excess gas in the bubbles is assumed to be released, from the bubbles, via the tunnels, to the pellet/sheath gap.

4.3 Diametral Changes and Circumferential Ridging

The following processes affect the diameter of the pellet and of the sheath: densification; swelling; creep; thermal expansion; and hourglassing.

Densification is caused by sintering of UO_2 in the reactor. It is calculated in ELESTRES as a function of: initial density of the pellet; local temperature; and time in the reactor. Swelling is caused by solid products of fission, which have a larger volume than the parent material, and by unreleased fission gases. Creep due to external coolant pressure decreases the diameter of the sheath. However, outward creep of sheath can be expected if the internal gas pressure significantly exceeds the coolant pressure.

Hourglassing of pellets is assumed to be caused by two factors: non-uniform temperature along the radius of the pellet; and axial compression.

The temperature profile along the pellet radius is, approximately, parabolic. Hence the thermal expansion does not produce the same radial displacement, or hoop strain, at adjacent radial locations. The resulting incompatibility causes stresses and strains that change radially and axially. The local strains and stresses are determined by, among others, the local stiffness of the pellet. At the pellet midplane, the deformation of a transverse cross-section is resisted not only by the stiffness of that cross-section, but also by the stiffness of the neighbouring UO_2. However, near the pellet end, the transverse cross-section is surrounded by less UO_2. Therefore it can, and does, expand more than the cross-section at the pellet midplane. The pellet thus takes the shape of an hourglass. This is one reason for circumferential ridges.

The amount of hourglassing is affected by many other parameters, for example: the dimensions and shape of the pellet; the temperature profile; the amount of radial interaction between the sheath and the pellet; and the amount of cracking in the pellet.

Axial compression also contributes to hourglassing. When the pellet expands axially, there may be axial interaction between neighbouring pellets, and/or between the stack of pellets and the endcap. This causes compressive axial forces on each pellet. Hydraulic drag is another source of compressive axial forces. This adds to the hourglassing of the pellet. Axial compression has a larger influence on ridging if the force is applied near the surface of the pellet than towards the center.

4.4 Feedbacks

Most of the preceding processes interact, and influence each other. For example, thermal expansion of the pellet increases the interfacial pressure between the sheath and the pellet, which lowers the temperature of the pellet, which reduces the amount of thermal expansion. Similar examples can be constructed for fission gas release, for sheath strain, and for internal pressure. ELESTRES accounts for the interdependence of these parameters.

4.5 Material Properties

The following properties of UO_2 and of Zircaloy, are used in ELESTRES: thermal conductivity; specific heat; coefficient of thermal expansion; Young's modulus; Poisson's ratio; yield strength; plastic modulus; creep rate; and stress for fracture. For use in ELESTRES, the values of these properties were obtained largely from the MATPRO[9] data base. Many of the properties depend strongly on local temperature, especially the thermal conductivity of UO_2; the yield strength of UO_2; and the creep rates of UO_2 and Zircaloy. The creep strength of Zircaloy is also a function of hardening due to irradiation, and of changes in the microstructure of Zircaloy. This subject is addressed in more detail later.

4.6 Sub-Models

ELESTRES uses the following sub-models:

(a) Neutron flux: ELESTRES uses an equation fitted to the results of the neutron-physics code HAMMER[10]. The equation gives neutron flux as a function of element diameter, enrichment, and burnup.

(b) Heat transfer coefficient between the pellet and the sheath: Empirical model by Campbell, Borque, Deshaies, Sills and Notley[11].

(c) Equiaxed grain growth: Model by Hastings, Scoberg and Mackenzie[12].

(d) Columnar grain growth: Application of the equations suggested by Olander[13] for surface diffusion and for transport by vapour phase. Logarthmic average of the two is taken, as suggested by Buescher and Meyer[14].

(e) Fission gas release: Model by Notley and Hastings[7].

(f) Densification and swelling: Model by Hastings, Fehrenbach, and Hosbons[15].

(g) Creep of UO_2: Equations suggested by Armstrong[16].

(h) Creep of Zircaloy at about 300°C: Model by Hosbons, Coleman and Holt[17].

(i) Creep of Zircaloy above 350°C: Model by Sills and Holt[18].

(j) Stress-corrosion-cracking: Model by Penn, Lo and Wood[19].

5. CALCULATION METHODS

5.1 Code Input

ELESTRES assumes that the fuel element consists of a cylindrical tube of Zircaloy or of steel, containing a stack of UO_2 pellets (steel is used in some experimental fuel). A plenum may also be included. The tube is sealed at both ends. The pellets may be solid or annular, dished or undished, or may be chamfered. The pellets may also contain grooves for instrumentation. The user specifies the details of the pellet and of the sheath, such as: geometry; dimensions; clearances, density; grain size; surface roughness; type of CANLUB coating; and enrichment. The user also specifies the composition and the pressure of the filling gas. The temperature and the pressure of the coolant are specified as a function of time. The power history is specified in terms of linear heat generation rate vs burnup.

5.2 Calculation Procedure

The power history is divided into a series of increments of powers and of burnups. A separate calculation is done for each increment. ELESTRES contains several features that permit large increments. These include: a special formulation for permitting many finite elements to simultaneously cross the boundary[20] from elastic to plastic behaviour; accomodation of large drops in yield-strength due to changes in local temperature[3]; and a three-step predictor/ corrector method for elastic/plastic analyses. These features reduce computing costs. For typical irradiation-histories (powers up to 80 kW/m, burnups up to 300 MW.h/kgU), ELESTRES requires less than one minute of computing time on a CDC/CYBER 175 computer.

6. TEMPERATURES

For temperatures, one-dimensional calculations are done in ELESTRES. That is, heat flow is considered along the radial direction, but not along the length, nor around the circumference.

When the power is held constant for a long time, say for more than one hour, ELESTRES calculates steady-state temperatures. These calculations use the finite difference method, and have already been described in Reference 1. But transient effects can also be important for some short-term situations, e.g. for postulated transients involving loss of control of reactivity. Hence, an option permits calculations of transient temperatures.

The following classical equation describes transient conduction of heat[21]:

$$k \frac{\partial^2 T}{\partial r^2} + \frac{k}{r} \frac{\partial T}{\partial r} + w = \rho s \frac{\partial T}{\partial t}$$

Here, k is thermal conductivity, T temperature, r radial distance, w rate of heat generation per unit volume, ρ density, s specific heat, and t time.

The equation is solved by dividing the pellet into a number of concentric annuli, usually 100. Another annulus represents the sheath, and one annulus models the gap between the sheath and the pellet. Within each annulus, the temperature is assumed to vary parabolically with distance. An implicit, incremental formulation of the above equation is obtained by using the one-step, Euler, backward-difference formula[21]. The incremental equations are formulated for each annulus. They are non-linear, because the thermal conductivity of UO_2 depends strongly on the local temperature. The equations for individual annuli are assembled into a matrix, to represent all the annuli simultaneously. This system of equations is solved iteratively, employing the modified Newton-Raphson scheme. The iterations continue until the net flow of heat has a low residual error at each time-step.

7. SHAPES OF FINITE ELEMENTS

The finite element method is used for calculating deformations, stresses, and strains, in pellets and in sheaths. Finite elements are available in two basic shapes: triangles, and rectangles. It is easier to formulate the stiffness matrix of rectangular elements than of triangles; the difference is especially noticeable in elements of higher order. Rectangles are also easier to use, because the nodes generally lie on grid-lines, and because the lines that connect the nodes are parallel to the coordinate axes. Below, we compare the accuracies of the two types of elements.

The stiffness matrix of a rectangular element can be generated by first dividing the rectangle into four triangles connected at the centroid of the rectangle, and then adding the stiffnesses of the four triangles[22]. Hence, for purposes of accuracy, a rectangular element is equivalent to four triangles assembled into a rectangular shape.

Udoguchi et. al.[23] have studied the accuracy of the solution vs the pattern into which individual finite elements are arranged. They considered plane-stress problems. They used Taylor series to represent the finite-element equations, and determined the discretization error of the series as a function of spacing between nodes. They found that when triangular elements are arranged in a rectangular pattern, the solution converges slowly. Also, it always retains a residual error. However, if triangular finite elements are assembled into a hexagonal pattern, the solution converges rapidly to the true solution. This is because the two patterns compensate differently for shear.

We checked if the theoretical results of Udoguchi et. al. have a significant effect on stresses in pellets. We modelled a solid cylinder experiencing a parabolic distribution of temperature along its radius.

We calculated the axisymmetric stresses due to the temperature-gradient. Figure 3a shows the calculated stresses when the elements were arranged in a rectangular pattern, Figure 3b for the hexagonal pattern. Compared to analytical solutions, the rectangular pattern, hence rectangular elements, provide reasonable predictions for hoop and axial stresses, but the radial stresses show large scatter. The hexagonal pattern, Figure 3b, gives better predictions for all three components, and the scatter is negligible. Also, the complex profile of the pellet near chamfers/dishes can be more easily recreated by assembling triangles than by assembling rectangles. For these reasons, ELESTRES avoids rectangular elements, and uses triangular elements arranged in a hexagonal pattern.

6. MULTIAXIAL STRESSES IN THE SHEATH

The failure rate is very low[5] in current CANDU fuel, which contains a layer of CANLUB. In the past, however, fuel failures have been reported[19] at circumferential ridges, and related to stress-corrosion-cracking during power-ramps. This problem was eliminated by introducing a layer of CANLUB, which reduces the exposure of the sheath to fission products, and by changing to new fuel-management schemes that give low stresses in the sheath. In addition, we developed a method of calculating sheath stresses, so that stresses can be kept low via suitable design and operating procedures.

The dominant source of stresses on the sheath, is expansion and hourglassing of the pellet. ELESTRES uses a finite element model for calculating hourglassing of the pellet. Elasticity, plasticity, creep and cracking are considered. The pellet is represented by 50-60 triangular finite elements assembled into a hexagonal pattern, see Figure 4. Reference 1 describes the details of this model.

During the irradiation, the sheath develops primary and secondary stresses. The primary stresses depend on factors like: coolant pressure; fission gas pressure; and hydraulic drag; see Figure 5. The primary stresses are mainly in the hoop and in the axial directions.

For normal values of element power the pellet expands more than the available radial clearance between the sheath and the pellet. This leads to secondary stresses in the sheath. Because of hourglassing, the stresses are higher near the circumferential ridge than near the midplane of the pellet. This generates in the sheath, hoop, bending (axial), shear, and radial stresses. Additional secondary axial stresses arise from axial interaction between neighbouring pellets, and from axial interaction between the endcap and the stack of pellets. All the secondary stresses relax rapidly due to creep.

Traditionally, one considers only the hoop strain in the sheath. But a more detailed study using the FEAST code showed[6] that near the ridge, the strains are highly multiaxial. The multiaxiality makes a significant difference to the level of stresses. For example, if other components of stresses were not present, the hoop stress cannot exceed the uniaxial tensile yield strength. But because of multiaxiality, the maximum hoop stress can be significantly higher than the uniaxial tensile yield strength. In addition, all components of stresses contribute to damage of the sheath. For example, Reference 6 investigates the influence of multiaxiality, on the fatigue of the sheath, during

power-cycling. The conclusion is that when the entire stress-system is applied on the sheath, the cycles to failure are half of those when only the hoop stress is applied.

We have therefore opted for multiaxial, axisymmetric, elastic-plastic calculations of stresses/strains in the sheath near the ridge. These calculations account for the axial variations in displacements/strains/stresses of the sheath, due to: pellet expansion and hourglassing; internal gas pressure; coolant pressure; and axial interactions. To do this, we solve the multiaxial classical equations describing the following fundamental laws of mechanics: equilibrium; compatibility; constitutive relations; yield criterion; and flow rule. The solution is obtained via the FEAST[3] code, hence these calculations are similar to those for pellet deformation[1]. Reference 3 gives a more detailed description of the method of solution.

Figure 5 shows a typical mesh in the sheath. The sheath contains a finer mesh than the pellet; this reflects the need to know detailed local variations in the sheath. The mesh in the sheath is tied to the mesh of the pellet; this precludes the need for interpolations and extrapolations. The study reported in Reference 6 showed that strains can change rapidly along the thickness of the sheath, and along its length. Because of the importance of stresses near the ridge, we use 5-7 nodes across the thickness at that location. Stresses are less critical near the midplane of the pellet, so 2-3 nodes are sufficient there. The comparatively coarse mesh near the midplane helps reduce computing-cost. The transition from big to small elements is gradual; this prevents the larger elements from dwarfing the stiffnesses of neighbouring smaller elements. For maximum accuracy, the aspect ratio is kept close to 1. The sheath is usually represented by about 200 nodes, forming about 300 triangular finite elements in a hexagonal pattern. Our experience shows that this combination gives sufficient accuracy at low cost.

9. CREEP OF SHEATH AT HIGH TEMPERATURES

Stresses lead to creep of the sheath. Anisotropy of the sheath plays an important role in the rate of creep. At temperatures near 300°C, the rate of creep of Zircaloy is calculated from the model by Hosbons, Coleman and Holt[17]. This model considers athermal and thermal creep due to changes in dislocation densities, and the effect of irradiation. Reference 1 describes the application of this model to ELESTRES.

For off-normal conditions, the temperature of the sheath may be significantly higher than 300°C. Then, the above model is not adequate, and ELESTRES uses the model by Sills and Holt[18]. This model is applicable for temperatures above 350°C, and accounts for creep due to:

- thermal and athermal strains due to changes in dislocation densities,
- diffusional creep due to sliding at grain boundaries, and
- transformation strain: During the transition of Zircaloy from α to β-phase, the crystal lattice expands its volume.

The rate of creep from the above three components depends on: temperatures; stresses; and microstructures of Zircaloy. Temperatures and stresses have already been discussed. The following paragraph summarizes the three major microstructural parameters considered in ELESTRES: recrystallization; fractions of α and β phases; and grain size.

Recrystallization, or annealing, occurs in Zircaloy above $\sim$ 430°C. Within the old grains, nucleation and growth of recrystallized grains give areas with low densities of dislocations. These areas grow thermally, thus annealing the material. The rate of removal of dislocations is estimated from the empirical model by Sills and Holt[18]. The distribution of α and β phases depends on the temperature and is obtained from the phase diagram. The size of grains is also a function of temperature. It is obtained from an empirical correlation based on microscopic examinations of fuel sheaths after heating to various temperatures. Further details of the creep model are available from Reference 18.

10. VALIDATION

Many of the physical processes are represented in ELESTRES by the same models as in ELESIM. The major difference is that the interactions among the sub-models are arranged slightly differently, and that some models are new in ELESTRES (e.g. hourglassing). Comparisons for about 80 irradiations show that, as expected, ELESTRES and ELESIM predict similar temperatures in the pellet. Hence, previous validations of ELESIM also apply to ELESTRES, for processes that are driven largely by temperatures: porosity; columnar and equiaxed grain-growth; size of grains; fission gas release.

Reference 1 compared the predictions of ELESTRES, against measurements of fission gas release (15 irradiations), and of sheath strains at circumferential ridges (10 irradiations). The data base covered element powers of 50-120 kW/m, and burnups of 1-300 MW.h/kgU. On average, the predictions of ELESTRES differed from measurements, by 1.3 percentage points for percent release of fission gas, and by 0.2 percentage points for hoop strain in the sheath. The newer version of ELESTRES has now been compared against about 80 irradiations in experimental reactors and in commercial reactors. The predictions continue to show reasonable agreement with measurements, see Figure 6. The next two sections present two more validations of ELESTRES against irradiation data: element ABS and bundle GB.

10.1 Element ABS

Element ABS was irradiated[24] for about one month at Chalk River Nuclear Laboratories, Canada. The power ranged from 30 to 60 kW/m. Hoop strain in the sheath was measured during the irradiation, using the In-Reactor Diameter Measuring Rig (IRDMR). Figure 7 shows the power history. It also compares the predictions of ELESTRES vs the measurements for hoop strains at the ridge, as a function of time. On average, the predictions compare well with measurements.

10.2 Bundle GB

In this experiment[25], the outer element was irradiated at powers between 48 and 75 kW/m, to a burnup of 300 MW.h/kgU. Figure 8 shows that the predictions of ELESTRES are within the ranges of post-irradiation measurements, for hoop strains at circumferential ridges.

11. ILLUSTRATIVE EXAMPLES

Reference 6 discusses some previous applications of ELESTRES. Below, we present two illustrative examples. They do not necessarily represent conditions in fuel elements in experimental or in commercial CANDU reactors. Rather, the intent here is to demonstrate some capabilities of the code that are not apparent from the previous section on validation.

The first example shows the patterns of stresses and strains during an increase in power. Figure 9 shows the elastic/plastic stresses near the ridge, for a power-boost of 40 kW/m at 140 MW.h/kgU. The multiaxiality of stresses is apparent. The axial stress shows sharp gradients across the thickness of the sheath. The shear stress shows significant variations along the length of the sheath. The maximum principal stress is 500 MPa. This, however, relaxes rapidly due to creep.

Figure 10 shows the distribution of elastic strains near a circumferential ridge, formed by a short-length-pellet, at a power of 56 kW/m at zero burnup. At the inner surface, the hoop and shear strains have similar magnitudes. At the outer surface, shear strains are low, but the axial strain is significant. The radial strain is compressive, but the absolute magnitude of peak radial strain is similar to that of hoop and shear strains. Thus, all four components contribute significantly to yield, creep, fatigue, and brittle fracture of the sheath.

The second illustrative example involves a Loss-of-Reactivity-Control accident (LORA). An excursion of power, at 80 MW.h/kgU, gradually increases the power by 18%. The coolant is maintained at full system pressure, but the overpower is assumed to cause dryout, which results in a low coefficient of heat transfer between the sheath and the coolant. Conservatively, we further assume that the drypatch covers the entire element: all around the circumference, and all along the length. These assumptions are not realistic, but nevertheless used here to show that the code can be used for simulating transients such as LORAs. Figure 11 shows the prediction of ELESTRES, for sheath hoop strains near the ridge and near the midplane of the pellet. During the transient, the elevated temperatures in the pellet increase the hoop strain at the ridge. The ridge height also increases.

12. SUMMARY AND CONCLUSIONS

(1) An improved version of ELESTRES is available for modelling the performance of nuclear fuel elements. The two-dimensional, axisymmetric calculations account for radial and axial variations.

(2) For given conditions of design and irradiation, the values of following parameters can be calculated by ELESTRES: temperatures, fission gas pressure, circumferential ridging, sheath stresses, and probability of failure due to stress-corrosion-cracking.

(3) Temperatures are calculated by one-dimensional models. The standard finite-difference method is used for steady-state temperatures, using 100 nodes across the radius. Transient temperatures use an implicit formulation and an iterative Newton-Raphson method.

(4) The finite element method is used for two-dimensional, axisymmetric calculations of displacements, stresses, and strains in the pellet and in the sheath. The pellet is represented by 40-50 finite elements, sheath by 200-300 elements. Elasticity, plasticity, creep and cracking are considered. Above 350°C, creep of Zircaloy is calculated from a model that considers diffusional creep, and dislocation-climb. This model accounts for changes in the microstructure of Zircaloy, such as grain-size, and fraction of α and β phases. Special numerical techniques keep the computing time below 1 minute on a CDC/CYBER 175 computer.

(5) Triangular finite elements arranged in a hexagonal pattern, give better accuracy than rectangular elements.

(6) ELESTRES shows good agreement with measurements of fission gas release, from $\sim$ 80 irradiations. The code also predicts well, sheath strains at circumferential ridges in experiments ABS and GB.

(7) Illustrative examples show a high degree of multiaxiality in stresses and in strain. The stresses/strains change rapidly with distance along the length of the sheath, and along the thickness.

13. ACKNOWLEDGEMENTS

The author gratefully acknowledges the encouragement, support, and contributions of R. Sejnoha, M. Gacesa, J.C. Wood, P.J. Fehrenbach, A. Banas, V.C. Orpen, D.R. Pendergast, J.K. Biswas, C.W. So, P.N. Singh, H.E. Sills, and J. Bunge. ELESIM, the starting point for ELESTRES, was developed largely by M.J.F. Notley. Special thanks to the H.E. Sills (CRNL), for his permission to include in this paper, some of his unpublished results (Fig. 6). The author also thanks COG (CANDU Owners Group) for funding the maintenance of ELESTRES, as part of the 'Operating Fuel Technology' program. The current members of COG, for 'Operating Fuel Technology', are: Ontario Hydro, Atomic Energy of Canada Limited, Hydro Quebec, and New Brunswick Electric Power Corporation.

14. REFERENCES

(1) H.H. Wong, E. Alp, W.R. Clendening, M. Tayal, L.R. Jones, "ELESTRES: A Finite Element Fuel Model for Normal Operating Conditions", Nuclear Technology, 57 (1982) 203-212.

(2) C.E. Coleman, D. Mills, J. Van der Kurr, "Deformation Parameters of Neutron Irradiated Zircaloy-4 at 300°C", Canadian Metallurgical Quarterly, II (1972) 91-100.

(3) M. Tayal, "FEAST: A Two-Dimensional Non-Linear Finite Element Code for Calculating Stresses", Seventh Annual Conference, Canadian Nuclear Society, 1986.

(4) H.E. Sills, "ELOCA: Fuel Element Behaviour During High-Temperature Transients", Atomic Energy of Canada Limited, Report AECL-6357, 1979.

(5) P.T. Truant, "CANDU Reactor Experience: Fuel Performance", Sixth Annual Conference, Canadian Nuclear Society, 1985.

(6) M. Tayal, "Recent Uses of the Finite Element Method in Design/Analysis of CANDU Fuel", Sixth Annual Conference, Canadian Nuclear Society, 1985.

(7) M.J.F. Notley, I.J. Hastings, " Microstructure-Dependent Model for Fission Product Release and Swelling in UO_2 Fuel", Nuclear Engineering and Design, 56 (1980) 163-175.

(8) A.H. Booth, "A Method of Calculating Fission Gas Diffusion from UO_2 Fuel and Its Application to the X-2-f Loop Test", Atomic Energy of Canada Limited, Report AECL-496, 1957.

(9) D.L. Hagrman, G.A. Reymann, "MATPRO - Version II: A Handbook of Material Properties for Use in The Analysis of Light Water Reactor Fuel Rod Behaviour", EG & G Idaho, Inc., Report NUREG/CR-0497, TREE-1280, R3, 1979.

(10) J.E. Suich, H.C. Honeck, "The HAMMER System", Savannah River Laboratories, Report DP-1064, 1967.

(11) F.B. Campbell, L.R. Bourque, R. Deshaies, H.E. Sills, M.J.F. Notley, "In-Reactor Measurement of Fuel-to-Sheath Heat Transfer Coefficients Between UO_2 and Stainless Steel", Atomic Energy of Canada Limited, Report AECL-5400, 1977.

(12) I.J. Hastings, J.A. Scoberg, K. Mackenzie, "Grain Growth in UO_2: In-Reactor and Laboratory Testing", Atomic Energy of Canada Limited, Report AECL-6411 (1979).

(13) D.R. Olander, "Fundamental Aspects of Nuclear Reactor Fuel Elements", ERDA Report TID 26711 (1976).

(14) B.J. Buescher, R.O. Meyer, J. Nucl. Mater., 48 (1973) 143.

(15) I.J. Hastings, P.J. Fehrenbach, R.R. Hosbons, "Densification in Irradiated UO_2 Fuel", Communications of the American Ceramic Society, Vol. 67, No. 2, p C-24, 1984.

(16) W. Armstrong, "Creep Deformation of Stoichiometric Uranium Oxide", J. Nucl. Mater., 7 (1962) 133.

(17) R.R. Hosbsons, C.E. Coleman, R.A. Holt, "Numerical Simulation of Tensile Behaviour of Nuclear Fuel Cladding Materials", Atomic Energy of Canada Limited, Report AECL-5245, 1975.

(18) H.E. Sills, R.A. Holt, "Predicting High Temperature Transient Deformation from Microstructural Models", ASTM STP 681 (1978) 325-341.

(19) W.J. Penn, R.K. Lo, J.C. Wood, "CANDU Fuel - Power Ramp Performance Criteria", Nuclear Technology, 34 (1977) 249.

(20) M. Tayal, D. Budney, "Load Increment Ratios in the Elastic-Plastic Analysis of Anisotropic Materials by the Variable-Stiffness Finite-Element Method", J. Strain Analysis, 11, 3, (1976), 150-153.

(21) A.J. Chapman, "Heat Transfer", McMillan Publishing Co., New York, 1974.

(22) O.C. Zienkiewics, "The Finite Element Method in Structural and Continuum Mechanics", McGraw-Hill Book Company, 1967.

(23) T. Udoguchi, H. Okamura, T. Kano, Y. Nozue, "An Error Analysis of Various Finite Element Patterns", Bul. JSME, 16, 102 (1973) 1803-1813.

(24) P.J. Fehrenbach, P.A. Morel, "In-Reactor Measurement of Clad Strain: Effect of Power History", Atomic Energy of Canada Limited, Report AECL-6686, 1980.

(25) R.R. Meadowcroft, P.E. Hynes, M. Tayal, "Irradiation Behaviour of Prototype 37 Element CANDU Fuel at High Power", Bulletin of the American Ceramic Society, Vol. 57, No. 3, 1978, p. 361.

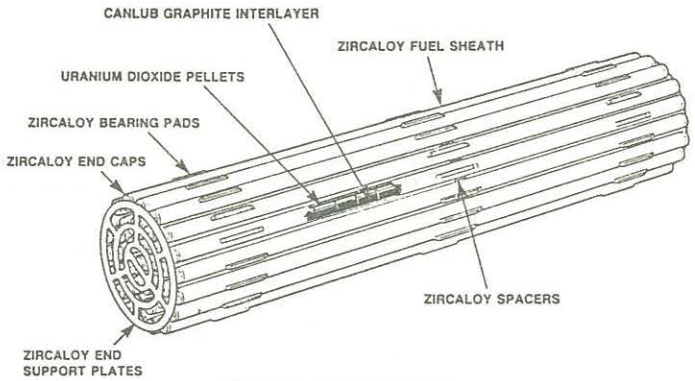

FIGURE 1 FUEL BUNDLE

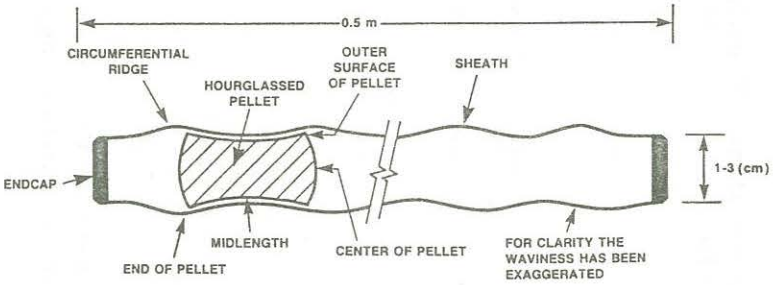

FIGURE 2 FUEL ELEMENT

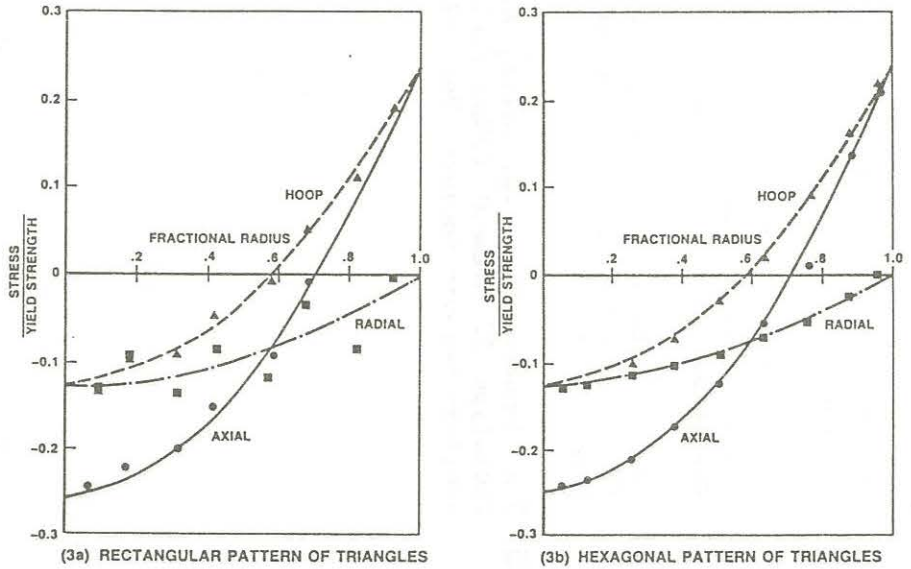

(3a) RECTANGULAR PATTERN OF TRIANGLES

(3b) HEXAGONAL PATTERN OF TRIANGLES

FIGURE 3 THERMAL STRESSES IN A CYLINDER: ANALYTICAL SOLUTIONS (LINES) VS FINITE ELEMENT CALCULATIONS (POINTS)

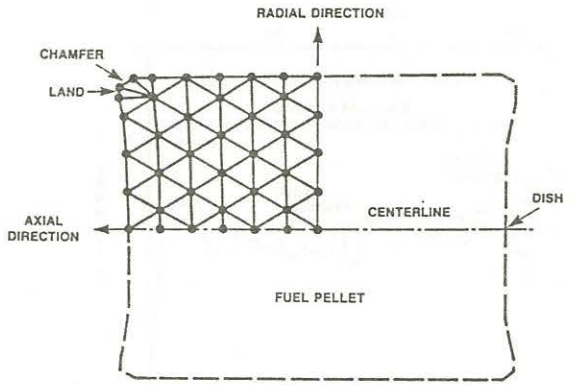

FIGURE 4 FINITE ELEMENT MESH IN THE PELLET

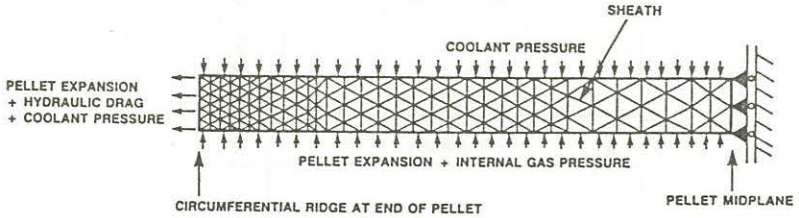

FIGURE 5 LOADS ON THE SHEATH, AND A FINITE ELEMENT MESH

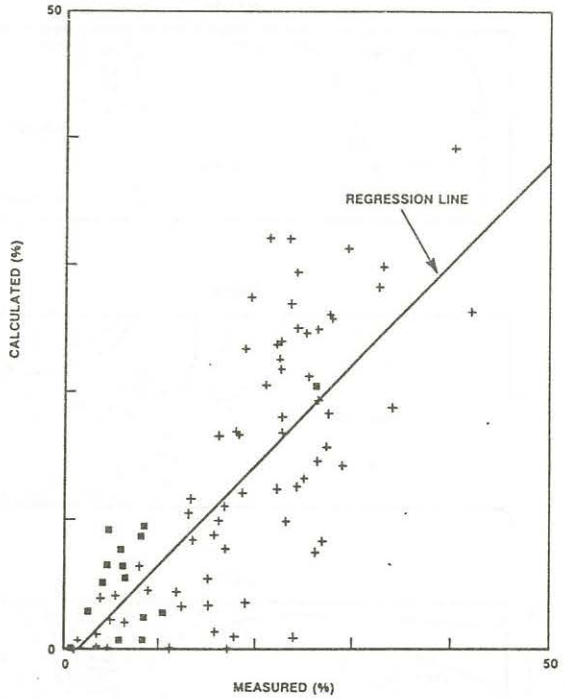

FIGURE 6 FISSION GAS RELEASE: MEASUREMENTS VS PREDICTIONS

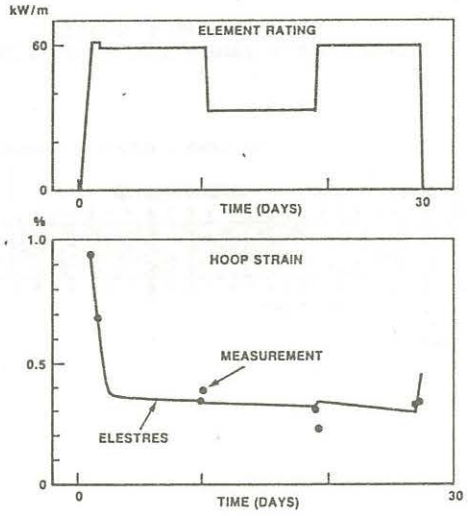

FIGURE 7 HOOP STRAIN AT THE RIDGE IN ELEMENT ABS: MEASUREMENTS VS ELESTRES

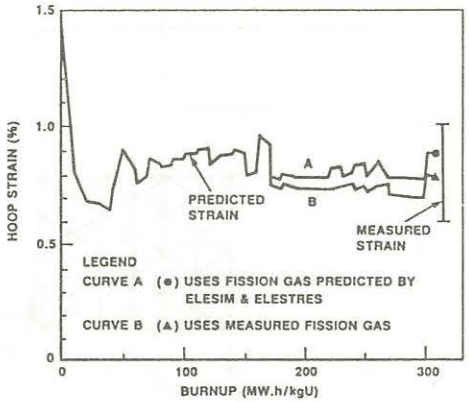

FIGURE 8 PLASTIC HOOP STRAIN AT CIRCUMFERENTIAL RIDGES IN BUNDLE GB: MEASUREMENTS VS ELESTRES

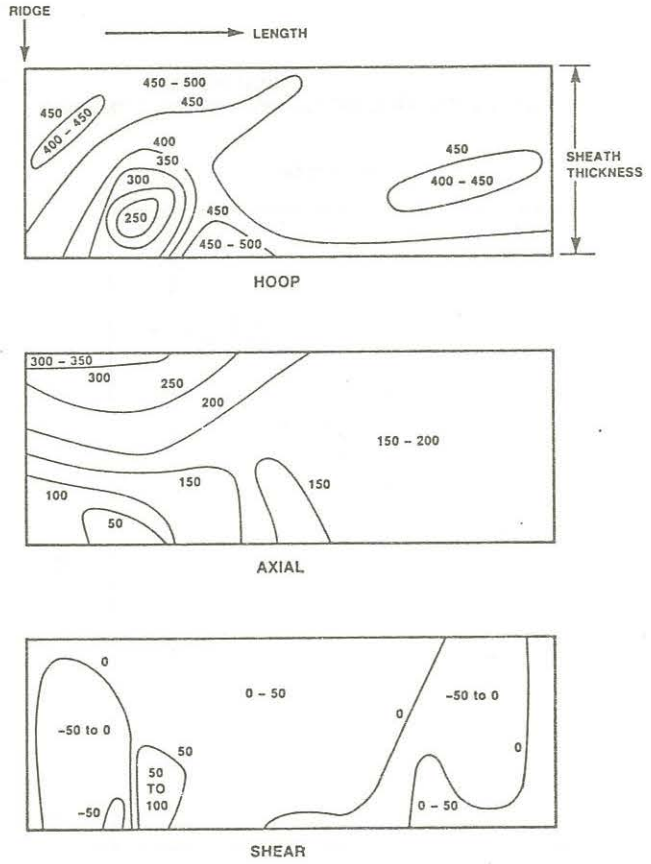

FIGURE 9 ELASTIC — PLASTIC STRESSES (MPa) IN THE SHEATH

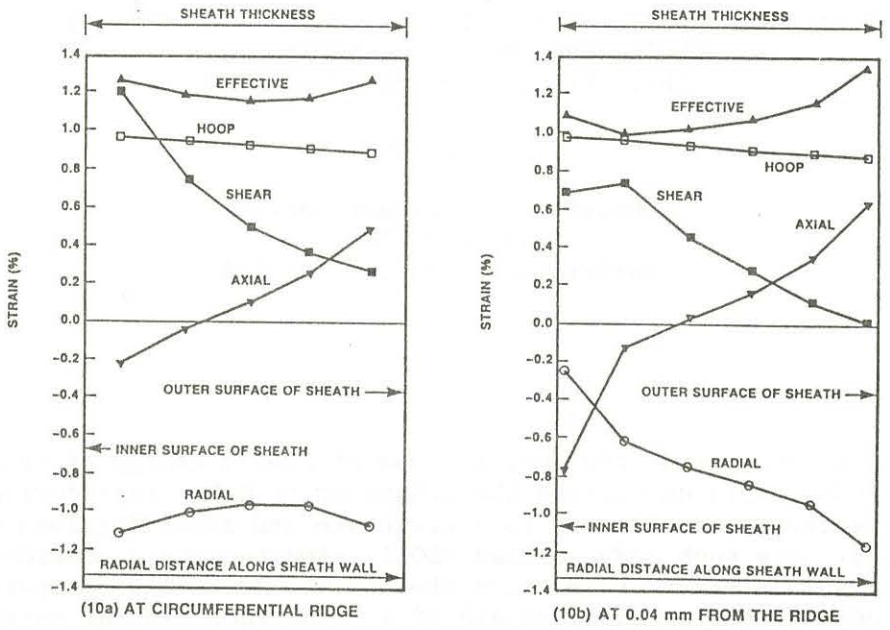

FIGURE 10 ELASTIC STRAINS ACROSS THE SHEATH WALL

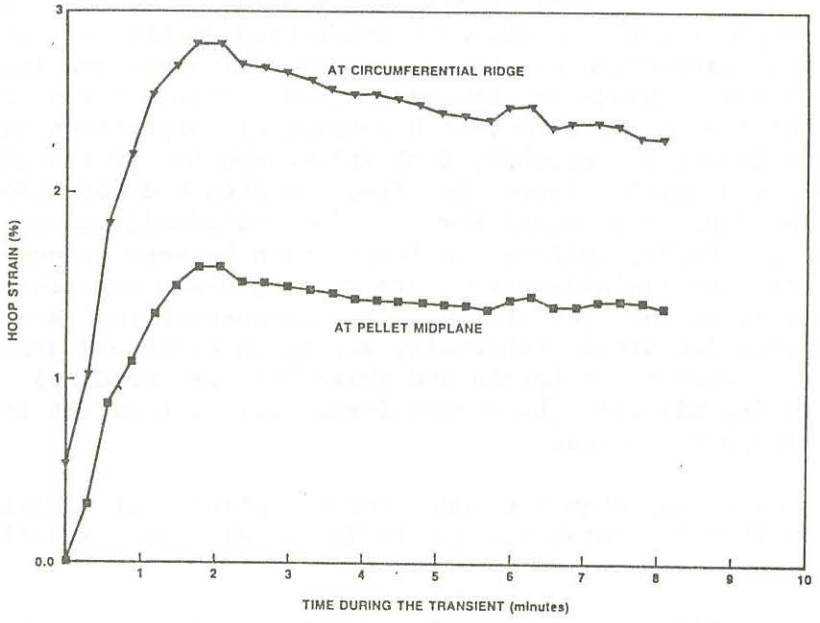

FIGURE 11 SHEATH STRAIN DURING A LOSS-OF-REACTIVITY-CONTROL ACCIDENT